Journal of Electrochemistry

Volume 27
Issue 2 *Special Issue of the Journal of Electrochemistry Celebrating 100 Years of Chemistry at Xiamen University (I)*

2021-04-28

Oxygen-Exposure Induced Rapid Oxidation of Spiro-OMeTAD in $CsPbIBr_2$ Perovskite Solar Cells

Wei-Guo Wang

Tian Bai

Gao-Fei Xue

Mei-Dan Ye
Research Institute for Biomimetics and Soft Matter, Fujian Provincial Key Laboratory for Soft Functional Materials Research, Department of Physics, College of Physical Science and Technology,Xiamen University, Xiamen 361005, Fujian, China;, mdye@xmu.edu.cn

第 27 卷 第 2 期
2021 年 4 月

电化学
JOURNAL OF ELECTROCHEMISTRY

Vol. 27 No. 2
Apr. 2021

【Article】 **DOI**: 10.13208/j.electrochem.201249 **Http**://electrochem.xmu.edu.cn

Oxygen-Exposure Induced Rapid Oxidation of Spiro-OMeTAD in $CsPbIBr_2$ Perovskite Solar Cells

Wei-Guo Wang, Tian Bai, Gao-Fei Xue, Mei-Dan Ye*

(*Research Institute for Biomimetics and Soft Matter, Fujian Provincial Key Laboratory for Soft Functional Materials Research, Department of Physics, College of Physical Science and Technology, Xiamen University, Xiamen 361005, Fujian, China*)

Abstract: 2,2′,7,7′-tetrakis(N,N-di-p-methoxyphenyl-amine)-9,9′-spirobifluorene (Spiro-OMeTAD) is the most widely used hole transport material in perovskite solar cells (PSCs). However, its oxidation in the air takes a long time and results in the attack of perovskite by water. In this regard, we performed the oxidation process of Spiro-OMeTAD in oxygen, where perovskite can be protected from water, guaranteeing the integrity of perovskite. It was demonstrated that the champion Spiro-OMeTAD based $CsPbIBr_2$ PSCs after oxygen oxidation achieved a 7.19% power conversion efficiency (PCE), showing a higher PCE than 6.29% of the champion device oxidized in air. A series of electrochemical characterization methods were applied to investigate the performances of the different cell devices under different oxidation conditions. It was revealed that the oxygen oxidation enabled to enhance the hole conductivity of Spiro-OMeTAD, reduce the charge recombination and improve the charge transfer efficiency in PSCs. Moreover, the device with oxygen oxidation had a higher average efficiency and greater stability. This method makes the devices have better repeatability, which provides a reliable idea for the commercial development of PSCs.

Key words: perovskite; Spiro-OMeTAD; rapid oxidation; $CsPbIBr_2$

1 Introduction

Organic-inorganic hybrid perovskite solar cells (PSCs) have made rapid progress in recent years. In 2009, the power conversion efficiency (PCE) of PSCs was only 3.8%[1]. Amazingly, after a short period of 11 years, the PCE of PSCs has reached more than 25% in 2020[2], which has attracted extensive attention of a considerable number of researchers. However, perovskite also has its own limitations, such as fear of water, heat, and light[3-6]. Encapsulation is an effective way to solve the problem of perovskite being afraid of water[7-9], but organic components will volatilize in a relatively hot environment, which is a huge obstacle to the commercialization of PSCs. Inorganic PSCs usually use inorganic Cs^+ instead of organic FA^+ or MA^+, so they have improved thermal stability. The excellent thermal stability of all inorganic perovskite shows great potential and upward development momentum[10-13]. To date, the best PCE of inorganic PSCs can reach over 18% based on the $CsPbI_3$ films, however, which still suffer from the stability problem due to the large ionic radius (2.2 Å) of I^-[14, 15]. Thus, Br^- with relatively smaller ionic radius (1.96 Å) is applied to partially replace I^- to form the $CsPbI_2Br$ or $CsPbIBr_2$ films[16, 17]. With careful modification on the devices, the PCE of $CsPbIBr_2$ PSCs can be over 11%[16, 18]. Moreover, all inorganic perovskite can not only operate independently as solar cells, but

Citation: Wang W G, Bai T, Xue G F, Ye M D. Oxygen-exposure induced rapid oxidation of Spiro-OMeTAD in $CsPbIBr_2$ perovskite solar cells. *J. Electrochem.*, 27(2): 216-226.

Received: 2021-02-04, Revised: 2021-03-17. *Corresponding author, Tel: (86)18859277190, E-mail: mdye@xmu.edu.cn

also form self-charging supercapacitors in series with supercapacitors[19], or drive efficient water splitting[20]. In addition to solar cells, all inorganic perovskite can also be used as photodetectors and light-emitting diodes[21, 22].

P-type semiconductor materials are frequently adopted as hole transport layers (HTLs) in PSCs. The participation of HTLs greatly improves the separation of electron-hole pairs and charge transfer efficiency of PSCs[23, 24]. Spiro-OMeTAD is one of the most widely used hole transport materials in PSCs. The conductivity of Spiro-OMeTAD itself is very low. The doping and oxidation of lithium salt (e.g., bis(trifluoromethane) sulfonimide lithium salt, LiTFSI) can improve the hole conductivity of Spiro-OMeTAD by two orders of magnitude based on the following reactions[25-27].

$$\text{Spiro-OMeTAD} + O_2 \leftrightarrow \text{Spiro-OMeTAD}\cdot^{+}O_2\cdot^{-} \quad (1)$$

$$\text{Spiro-OMeTAD}\cdot + O_2\cdot^{-} + \text{LiTFSI} \rightarrow \text{Spiro-OMeTAD}\cdot^{+}\text{TFSI}^{-} + Li_xO_y \quad (2)$$

However, the traditional method is to oxidize Spiro-OMeTAD in ambient conditions overnight, which exposes perovskite to dangerous moisture. Long time oxidation in the air may cause the oxidation quality of Spiro-OMeTAD to fluctuate greatly, and reduce the PCEs of PSCs. Researchers have developed several ways to replace such air oxidation process of Spiro-OMeTAD[28-30]. For example, a new hole transport material named $Spiro(TFSI)_2$ was synthesized, which can have good hole conductivity without air oxidation, and have higher efficiency and repeatability than the devices with air oxidation[30]. Oxygen/argon mixture plasma was applied to realize the rapid oxidation of Spiro-OMeTAD with high conductivity and mobility[28]. However, there are few studies about the effect of oxygen on Spiro-OMeTAD in organic perovskite solar cells. Liu et al. studied the effect of oxygen aging time on the performance of PSC devices, but only limited to the effect of aging time, and did not compare with devices oxidized in air[31].

In this work, we used pure oxygen to rapidly oxidize Spiro-OMeTAD in a short period of time. It not only improves the efficiency of PSCs, but also makes the quality of devices more stable and has better repeatability, which are important and indispensable for the commercialization of PSCs.

2 Experimental Section

2.1 Materials

Tin oxide (SnO_2) quantum dot solution (15wt.% in H_2O colloidal dispersion) was obtained from Alfa Aesar. The cesium iodide (CsI, 99.99%), lead (II) bromine ($PbBr_2$, 99.99%), 2,2′,7,7′-tetrakis(N,N-di-p-methoxyphenylamine)-9,9′-spirobifluorene (Spiro-OMeTAD, 99.8%), bis(trifluoromethane) sulfonimide lithium salt (Li-TFSI, 99%), and 4-tert-butylpyridine (TBP, 96%) were purchased from Xi'an Polymer Light Technology Corporation. DMSO (99.9%). Chlorobenzene (CB, 99.8%), and acetonitrile (99.8%) were purchased from Sigma-Aldrich. All the materials were used without further purification.

2.2 Device Fabrication

The indium tin oxide (ITO) substrate was cleaned in the ultrasonic instrument with detergent water, acetone, ethanol and deionized water in sequence. Then, the oxygen plasma cleaning step was applied for 20 min to further clean the substrate. Then, SnO_2 solution was spin-coated on the clean substrate as an electron transport layer (ETL) and annealed at 150 ºC for 30 min. Lead bromide ($PbBr_2$) and cesium iodide (CsI) were dissolved in DMSO at a stoichiometric ratio of 1:1 as a precursor solution. The $CsPbIBr_2$ precursor solution was spin-coated on the SnO_2 ETL at 3000 $r\cdot min^{-1}$ for 30 s. The resulting substrate was immediately transferred to a hot plate and annealed at 280 ºC for 30 min. The Spiro-OMeTAD solution was prepared by dissolving 72.3 mg of Spiro-OMeTAD, 28.9 μL of TBP, and 17.5 μL of a stock solution of 520 $mg\cdot mL^{-1}$ Li-TFSI in acetonitrile in 1 mL of chlorobenzene. The Spiro-OMeTAD solution was spin-coated at 3000 $r\cdot min^{-1}$ for 30 s. After the spin-coating process, the sample was immediately exposed to air or oxygen for the oxidation treatment. After oxidation, a 100 nm-thick Ag layer was deposited on the sample by evaporation.

2.3 Characterizations

The morphologies of perovskite films were observed by scanning electron microscope (SEM, Zeiss). The surface roughness of the perovskite film was tested by atomic force microscope (AFM Bruker MultiMode 8 scanning probe microscope). The crystal structure was examined by X-ray Diffraction (XRD, Panalytical X'pert Pro) with a CuK_α source. Steady PL spectra were recorded on a Fluorescence Spectrophotometer (Hitachi F-7000) with a 380 nm excitation. The photovoltaic *J-V* curves were measured under a solar simulator (500 W Model 91160, Newport) with an AM 1.5 spectrum (100 mW·cm^{-2}) to simulate a full sun intensity. The IPCE spectra were elucidated by a specially designed IPCE system (Enli Technology Co. Ltd) which was calibrated with a NIST-calibrated silicon photodiode G425 before each measurement. The IPCE results of the PSCs were collected as a function of wavelength from 300 to 1100 nm using a 75 W Xe lamp as a light source for generating monochromatic beam at a low chopping frequency. Electrochemical Impedance Spectroscopic (EIS) data was recorded on a CHI660E electrochemical workstation under a frequency range of 0.1 Hz ~ 100 kHz without bias-voltage. Intensity modulated photovoltage spectra (IMVS) were obtained by the CIMPS-PCS system (Zahner). The test light intensity was 50 W·cm^{-2}, the perturbation current was 10 mA, and the frequency was 0.1 Hz ~ 100 kHz.

3 Results and Discussion

The process of fabricating the cell devices is shown in Figure 1. The SnO_2 electron transport layer (ETL), $CsPbIBr_2$ and Spiro-OMeTAD were successively deposited on the ITO substrate by the one-step spin coating method. To figure out the effect of oxidation on Spiro-OMeTAD as a hole transport layer in PSCs, the similar devices with ITO/SnO_2/$CsPbIBr_2$/Spiro-OMeTAD were oxidized in the air and oxygen for different times, respectively. After oxidation, the Ag electrode was deposited by vacuum evaporation.

As shown in Figure 2(A), the $CsPbIBr_2$ film was compact without obvious pinholes, and the crystal sizes were not uniform ranging from 200 nm to 1 μm. AFM images (Figure 2(B)-2(C)) indicate that the average roughness of the film was 16.9 nm, suggesting that the film is smooth and compact. The XRD pattern of the $CsPbIBr_2$ film (Figure 2(D)) displays two strong diffraction peaks at 2θ = 14.83° and 30.00°, corresponding to the (100) and (200) planes of the $CsPbIBr_2$ perovskite, respectively[32, 33]. The absorption spectrum of the $CsPbIBr_2$ film (Figure 2(E)) exhibited the absorption around 600 nm with a band gap of 2.07 eV, which is similar to those of $CsPbIBr_2$ perovskites in literature[34, 35]. In addition, Figure 2(F)

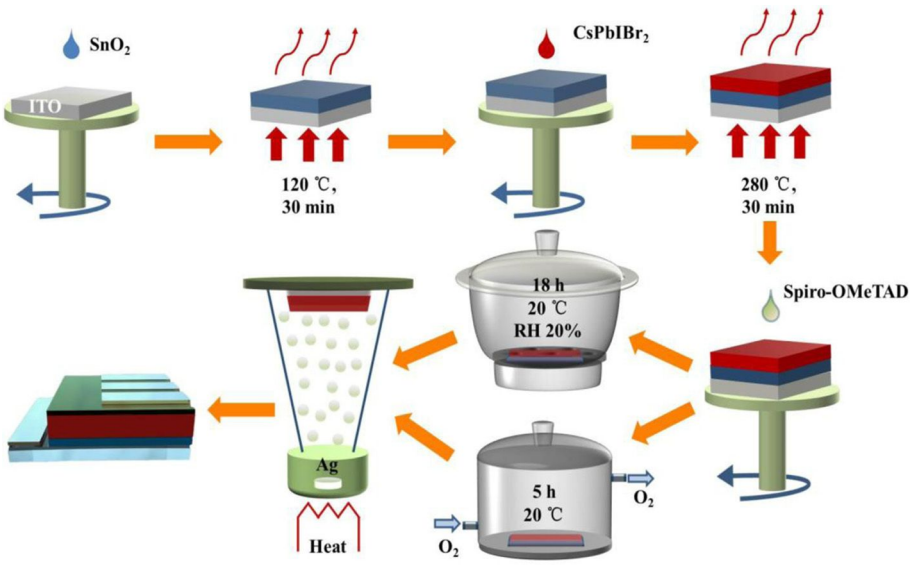

Figure 1 Fabrication of perovskite solar cells with the hole transport layer under different oxidation conditions. (color on line)

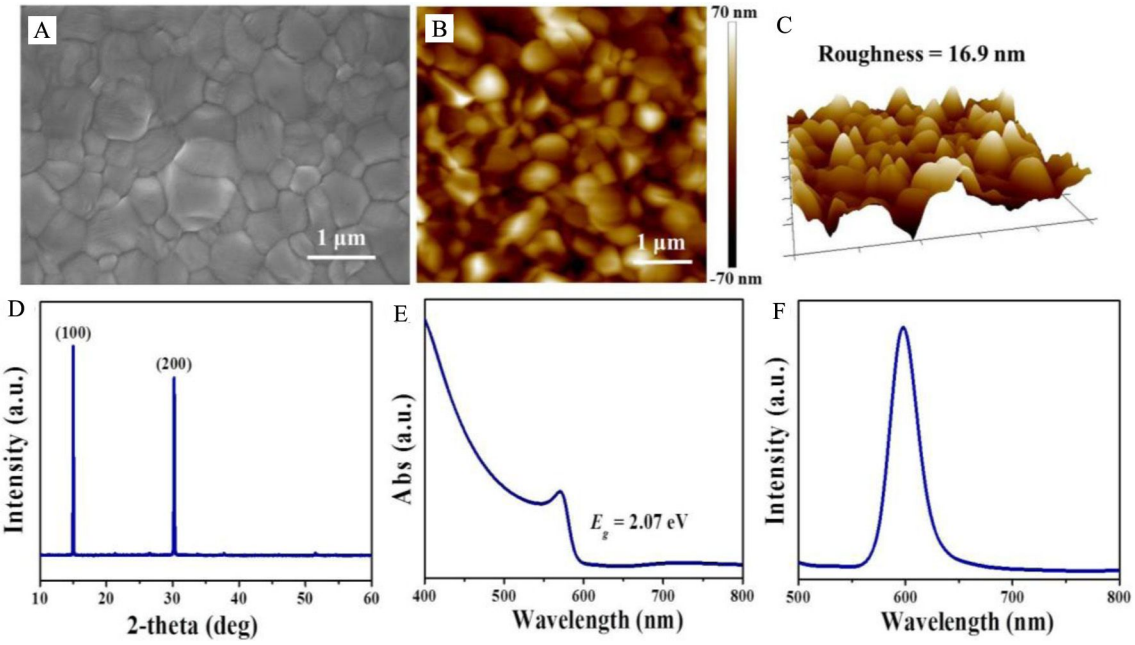

Figure 2 Characterizations of the $CsPbIBr_2$ films: (A) SEM image, (B) AFM plane graph and (C) three-dimensional graph, (D) XRD pattern, (E) UV-Vis absorption spectrum, and (F) normalized steady PL spectrum. (color on line)

shows the steady-state PL emission spectrum of the $CsPbIBr_2$ film, and the emission peak appears at about 600 nm, which is also consistent with the previous report[36].

Subsequently, the $CsPbIBr_2$ films were adopted to fabricate PSCs with the device structure of ITO/SnO_2/$CsPbIBr_2$/Spiro-OMeTAD/Ag. The PSCs were tested under 100 mW·cm^{-2} light and the obtained *J*-*V* curves are shown in Figure 3. Table 1 provides more detailed parameters of PSCs. The PSCs oxidized in the air environment reached the best performance after 18 h, yielding the PCE of 6.29%. Within a short oxidation time, the PCE of PSCs was low, which may be due to the insufficient oxidation of Spiro-OMeTAD, and the ineffective improvement of hole conductivity, resulting in low carrier mobility and increased contact resistance in devices. However, a long oxidation time was also detrimental to the device due mainly to the damage of perovskite exposed to moisture for a long time. Especially, the lithium salt in the Spiro-OMeTAD layer is hygroscopic, which makes the humidity have a greater impact on the device. On the contrary, the device oxidized in oxygen can prevent the moisture invasion. Moreover, the effect of oxygen on Spiro-OMeTAD showed faster feedback, and the champion efficiency of 7.19% could be achieved after merely 5 h oxidation. The PCE of the device oxidized in oxygen for 7 h decreased to 5.71%, which may be due to the partial decomposition of perovskite by oxygen[37, 38]. It indicates that PSCs should not be oxidized in oxygen for a long time. Particularly, O_2-5 h showed better performance than Air-18 h. On the one hand, it may be because that O_2-5 h perovskite retained a better crystal structure due to the oxidation process of isolating humidity. On the other hand, it has been reported that oxygen has a passivation effect on perovskite. Although oxygen can decompose perovskite, in a certain oxidation time range, the passivation effect of oxygen may play a dominant role, Moreover, all inorganic perovskite has more carrier defects than organic-inorganic hybrid perovskite, and oxygen passivation may be an effective method to improve the performance of devices[39-41].

The IPCE curves were respectively measured from champion devices with the air and oxygen treatments (Figure 4). In the whole wavelength range of photocurrent generation (300 ~ 620 nm), the EQE value

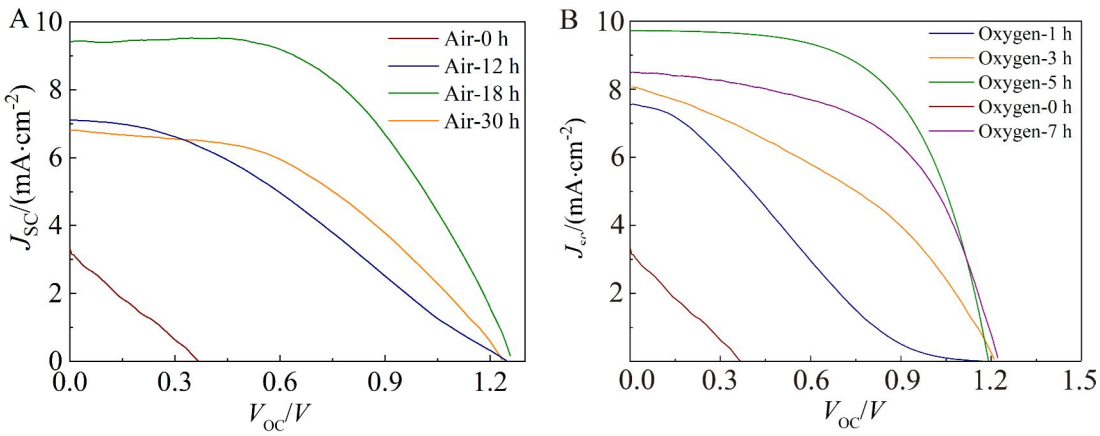

Figure 3 *J-V* curves of PSCs oxidized in the (A) air, and (B) oxygen. (color on line)

Table 1 The best parameters of PSCs oxidized under different conditions.

Device	PCE/%	V_{OC}/V	J_{SC}/(mA·cm^{-2})	FF/%	Area/cm^2
0 h	0.29	0.37	3.34	23.84	0.09
O_2-1 h	2.04	1.20	7.56	22.39	0.09
O_2-3 h	3.77	1.21	8.06	38.50	0.09
O_2-5 h	7.19	1.19	9.92	60.38	0.09
O_2-7 h	5.71	1.22	8.49	54.85	0.09
Air-12 h	2.99	1.24	7.10	33.7	0.09
Air-18 h	6.29	1.26	9.41	52.90	0.09
Air-30 h	3.77	1.23	6.80	44.75	0.09

of the O_2-5 h device was higher than that of the air-18 h device. According to the IPCE curves, the integral current density curves of the two devices were calculated. The integral short-circuit current density (J_{SC}) of the air-18 h cell was 9.33 mA·cm^{-2}, while that of the O_2-5 h cell was 10.08 mA·cm^{-2}, which is consistent with the results of *J-V* curves (Table 1).

EIS was adopted as a tool to track the electron transfer process of PSCs. The EIS diagrams and fitting circuits are shown in Figure 5. R_s is the series resistance related to the contact resistance, C_g is the geometric capacitance related to the bulk properties of perovskite[42, 43], C_s is the surface charge accumulation capacitance at the contact/perovskite interface[44], R_1 and R_2 are parameters related to the carrier coincidence process, and the total composite resistance is $R_s = R_1 + R_2$[45] From the fitting Nyquist diagrams

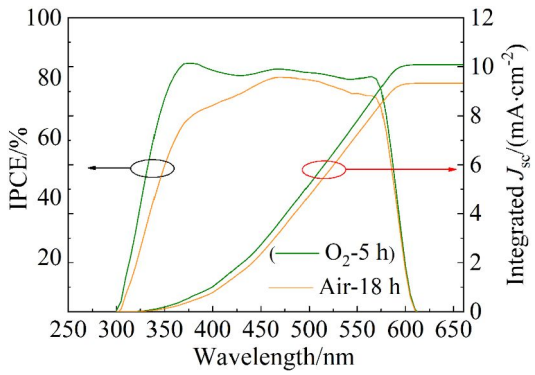

Figure 4 IPCE curves of the O_2-5 h and Air-18 h cells.(color on line)

(Figure 5), compared with other devices, the device without oxidation treatment shows greater total composite resistance, which may be due to the low carrier mobility of Spiro-OMeTAD itself[46]. The O_2-5 h de-

vice has the smallest R_s value, which means that compared with the O_2-1 h and O_2-3 h devices, there is less total resistance and less carrier recombination in the device. The reason may be that Spiro-OMeTAD has higher carrier transfer rate due to the more sufficient oxidation, which makes the O_2-5 h cell have faster charge extraction ability. In addition, relatively long time exposure to oxygen may passivate the defects in perovskite and reduce the nonradiative recombination of carriers in perovskite[3, 4, 31]. Compared with the air-18 h device (Figure 5), the O_2-5 h device has slightly smaller series resistance, which may be due to the air-18 h cell being eroded by water in the air.

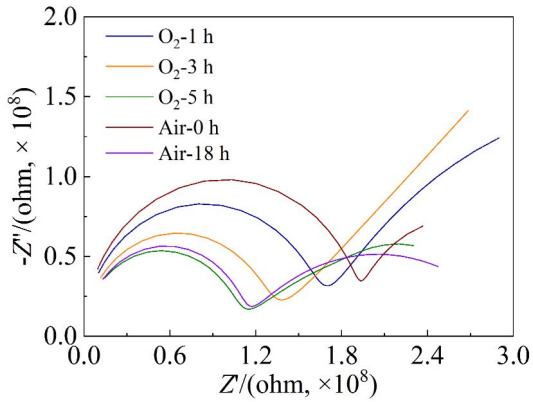

Figure 5 EIS data: EIS diagrams of PSCs oxidized in oxygen for different time compared with the air-0 h and air-18 h devices.(color on line)

To study the effect of different oxidation conditions on the charge recombination of the devices, the IMVS response of the devices was measured in the range of 0.1 Hz ~ 100 kHz under the amplitude current of 10 mA. According to the lowest frequency f_{min} obtained from the curves and the calculation formula: $\tau_n = 1/2\pi f_{min}$, the effective electron lifetime τ_n value of each device was obtained[47, 48]. The τ_n value of the O_2-5 h cell is 60.25 μs, while the τ_n values of the O_2-1 h and O_2-3 h cells are 30.57 μs and 24.35 μs, respectively, which indicates that the charge recombination in the device is reduced with the increase of oxidation time. Similarly, in the air condition, the τ_n value of the air-18 h device is 48.16 μs, while the τ_n values of the air-0 h, air-12 h and air-30 h devices are 6.23 μs, 15.46 μs and 30.57 μs, respectively. Thus, the oxidation process is able to reduce charge reobimnation and improves the charge transfer in the PSC devices.

To obtain more accurate and reliable results, the PCE, J_{SC}, V_{OC}(open circuit voltage), and *FF* (fill factor) values of 20 devices oxidized in the air and oxygen conditions are plotted in Figure 7 and in Figure 8, respectively. The summarized results indicate that the devices obtained from the oxygen condition have a higher average efficiency, and the PCEs of several devices exceed 6%, even up to 7%, which does not appear in the air oxidation group. It seems that the increase in the device efficiency is mainly related to the increases of J_{SC} and *FF*. Oxygen oxidation is beneficial to improve the hole conductivity of Spiro-OMeTAD, thus, the increase of J_{SC} may be related to this reason[49]. While the improvement of *FF* may be related to the

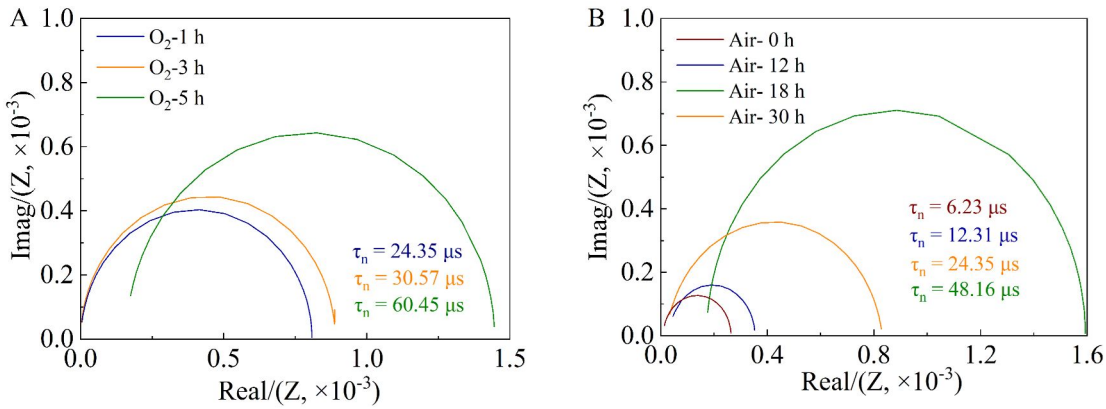

Figure 6 IMVS diagrams of (A) oxygen-exposed and (B) air-exposed PSCs. (color on line)

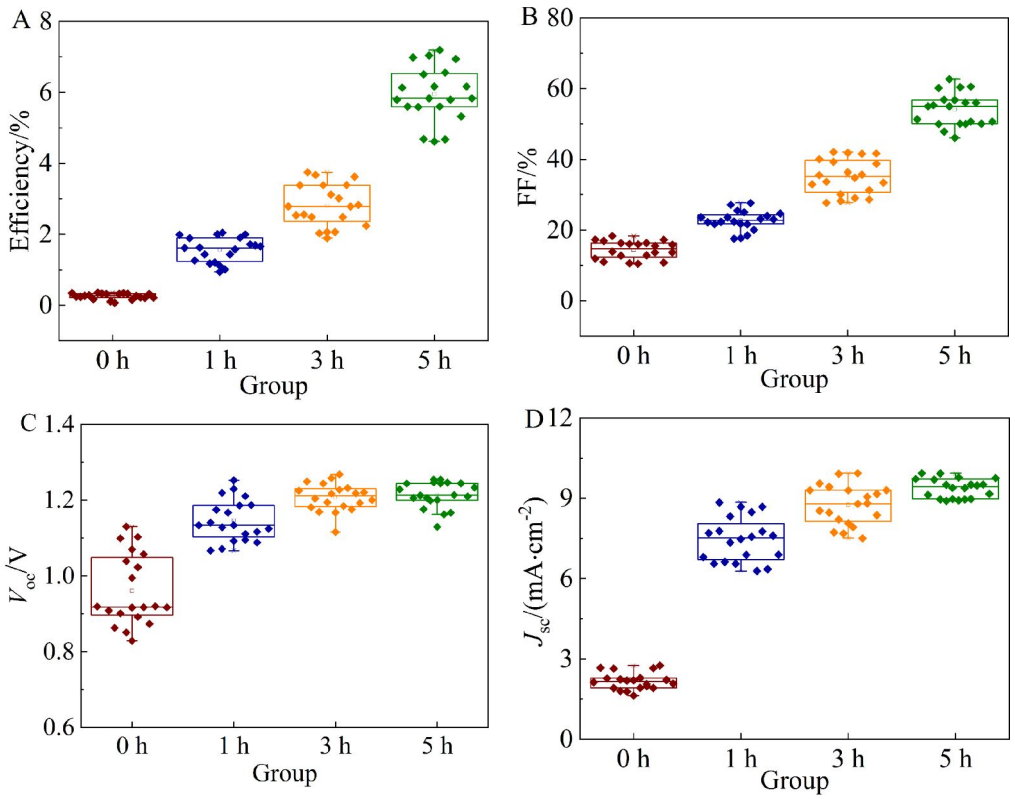

Figure 7 Device parameters of the oxygen-oxidized PSCs: (A) PCE, (B) *FF*, (C) V_{OC}, and (D) J_{SC} statistics. (color on line)

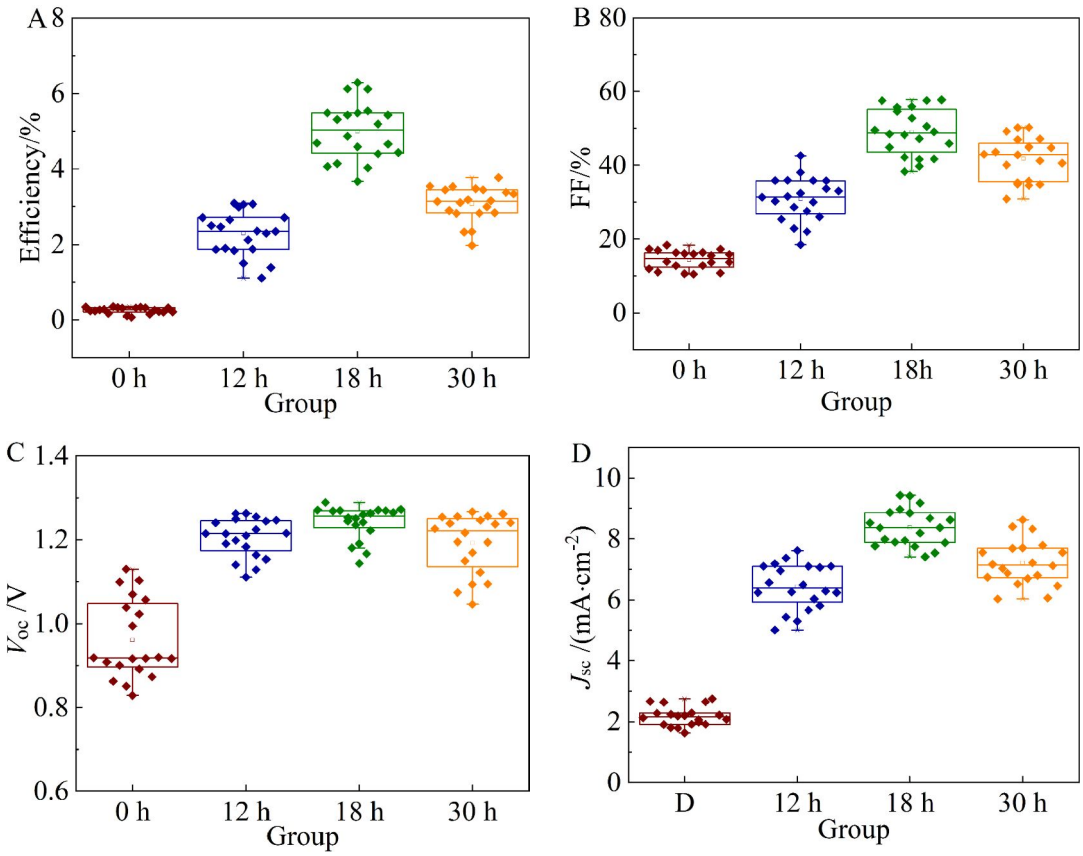

Figure 8 Device parameters of the air-oxidized PSCs: (A) PCE, (B) *FF*, (C) V_{OC}, and (d) J_{SC} statistics.(color on line)

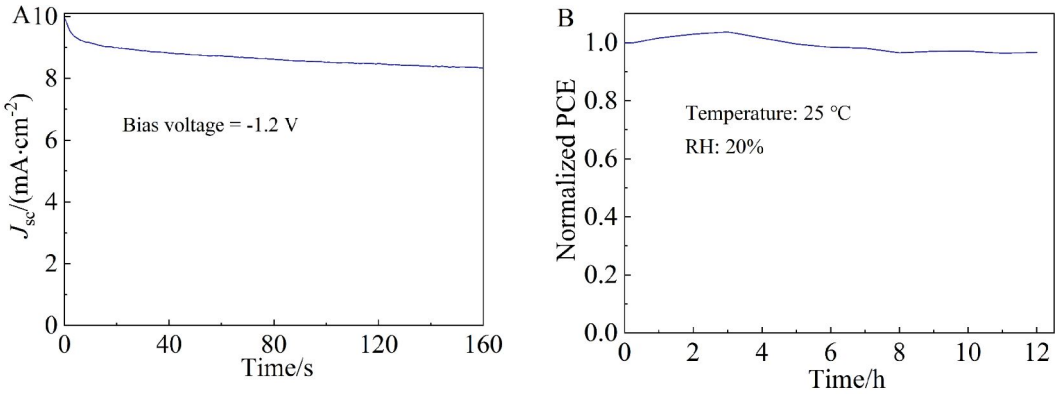

Figure 9 Time-dependent variations of (A) maximum J_{SC} under -1.2 V bias voltage, and (B) normalized PCE stored in 20% RH and 25 °C for the O_2-5 h device.

more efficient charge extraction[50]. In the air-oxidized cells, it is possible that the effect of oxidation is not the only factor on the performance of PSCs. The average efficiency of the cells after oxidation for 30 h is lower than that after oxidation for 18 h. This may be due to the decomposition of perovskite caused by the attack of water, which makes the perovskite layer itself produce more carrier complex traps, and worsens the contact between the perovskite layer and ETL/HTL, as well as increases the external series resistance, resulting in the decreases of J_{SC} and *FF* values[51, 52].

In addition, the stability of PSCs was tested as well. The change of J_{SC} under the bias of -1.2 V was measured, and no significant decrease was found. Then, the champion cell oxidized in oxygen for 5 h was stored in a desiccator with a humidity of 20% and the change of efficiency within 12 h under water erosion was detected. Fortunately, no obvious decrease was found within 12 h.

4 Conclusions

Inorganic PSCs with the ITO/SnO_2/$CsPbIBr_2$/Spiro-OMeTAD/Ag structure were fabricated. By controlling the oxidation time of Spiro-OMeTAD in the air and oxygen conditions, various electrochemical techniques were employed to study the device performance. It is found that due to the water erosion, the oxidation efficiency and average quality of the devices decreased based on the air oxidation. The devices oxidized in oxygen had higher efficiency, and, more importantly, better average quality because of no water interference, which provides an effective and reliable idea for the future industrialization of PSCs.

Acknowledgements

This work was supported by the National Science Foundation (No. 22075237).

References:

[1] Kojima A, Teshima K, Shirai Y, Miyasaka T. Organometal halide perovskites as visible-light sensitizers for photovoltaic cells[J]. J. Am. Chem. Soc., 2009, 131(17): 6050-6051.

[2] Sahli F, Werner J, Kamino BA, Bräuninger M, Monnard R, Paviet-Salomon B, Barraud L, Ding L, Diaz Leon J J, Sacchetto D, Cattaneo G, Despeisse M, Boccard M, Nicolay S, Jeangros Q, Niesen B, Ballif C. Fully textured monolithic perovskite/silicon tandem solar cells with 25.2% power conversion efficiency[J]. Nat. Mater., 2018, 17(9): 820-826.

[3] Bryant D, Aristidou N, Pont S, Sanchez-Molina I, Chotchunangatchaval T, Wheeler S, Durrant J R, Haque S A. Light and oxygen induced degradation limits the operational stability of methylammonium lead triiodide perovskite solar cells[J]. Energy. Environ. Sci., 2016, 9(5): 1655-1660.

[4] Pearson A J, Eperon G E, Hopkinson P E, Habisreutinger S N, Wang J T W, Snaith H J, Greenham N C. Oxygen degradation in mesoporous Al_2O_3/$CH_3NH_3PbI_{3-x}Cl_x$ perovskite solar cells: kinetics and mechanisms[J]. Adv. Energy Mater., 2016, 6(13): 1600014.

[5] Berhe T A, Su W N, Chen C H, Pan C J, Cheng J H, Chen H M, Tsai M C, Chen L Y, Dubale A A, Hwang B J. Organometal halide perovskite solar cells: degradation and

stability[J]. Energy Environ. Sci., 2016, 9(2): 323-356.

[6] Huang J, Tan S, Lund P D, Zhou H. Impact of H_2O on organic-inorganic hybrid perovskite solar cells[J]. Energy Environ. Sci., 2017, 10(11): 2284-2311.

[7] Dong Q, Liu F, Wong M K, Tam H W, Djurišic A B, Ng A, Surya C, Chan W K, Ng AMC. Encapsulation of perovskite solar cells for high humidity conditions[J]. ChemSusChem, 2016, 9(18): 2597-2603.

[8] Weerasinghe H C, Dkhissi Y, Scully A D, Caruso R A, Cheng Y B. Encapsulation for improving the lifetime of flexible perovskite solar cells[J]. Nano Energy, 2015, 18: 118-125.

[9] Matteocci F, Cinà L, Lamanna E, Cacovich S, Divitini G, Midgley P A, Ducati C, Di Carlo A. Encapsulation for long-term stability enhancement of perovskite solar cells [J]. Nano Energy, 2016, 30: 162-172.

[10] Ouedraogo N A N, Chen Y, Xiao Y Y, Meng Q, Han C B, Yan H, Zhang Y. Stability of all-inorganic perovskite solar cells[J]. Nano Energy, 2020, 67: 104249.

[11] Li B, Fu L, Li S, Li H, Pan L, Wang L, Chang B H, Yin L W. Pathways toward high-performance inorganic perovskite solar cells: challenges and strategies[J]. J. Mater. Chem. A, 2019, 7(36): 20494-20518.

[12] Liang J, Wang C X, Wang Y R, Xu Z R, Lu Z R, Ma Y, Zhu H F, Hu Y, Xiao C C, Yi X, Zhu G Y, Lü H L, Ma L B, Chen T, Tie Z X, Jin Z, Liu J. All-inorganic perovskite solar cells[J]. J. Am. Chem. Soc., 2016, 138(49): 15829-15832.

[13] Liang J, Zhao P Y, Wang C X, Wang Y R, Hu Y, Zhu G Y, Ma L B, Liu J, Jin Z. $CsPb_{0.9}Sn_{0.1}IBr_2$ based all-inorganic perovskite solar cells with exceptional efficiency and dtability[J]. J. Am. Chem. Soc., 2017, 139(40): 14009-14012.

[14] Wang Y, Dar M I, Ono L K, Zhang T Y, Kan M, Li Y W, Zhang L J, Wang X T, Yang Y G, Gao X Y. Thermodynamically stabilized β-$CsPbI_3$-based perovskite solar cells with efficiencies > 18%[J]. Science, 2019, 365(6453): 591-595.

[15] Chu W B, Saidi W A, Zhao J, Prezhdo O V. Soft lattice and defect covalency rationalize tolerance of β-$CsPbI_3$ perovskite solar cells to native defects[J]. Angew. Chem. Int. Ed., 2020, 59(16): 6435-6441.

[16] You Y B, Tian W, Wang M, Coo F R, Sun H X, Li L. PEG modified $CsPbIBr_2$ perovskite film for efficient and stable solar cells[J]. Adv. Mater. Interfaces, 2020, 7(13): 2000537.

[17] Chen W J, Chen H Y, Xu G Y, Xue R M, Wang S H, Li Y W, Li Y F. Precise control of crystal growth for highly efficient $CsPbI_2Br$ perovskite solar cells[J]. Joule, 2019, 3 (1): 191-204.

[18] Gao B W, Meng J. Highly stable all-inorganic $CsPbIBr_2$ perovskite solar cells with 11.30% efficiency using crystal interface passivation[J]. ACS Appl. Energy Mater. 2020, 3 (9): 8249-8256.

[19] Liang J, Zhu G Y, Wang C X, Zhao P Y, Wang Y R, Hu Y, Ma L B, Tie Z X, Liu J, Jin Z. An all-inorganic perovskite solar capacitor for efficient and stable spontaneous photocharging[J]. Nano Energy, 2018, 52: 239-245.

[20] Ma L B, Zhang W J, Zhao P Y, Liang J, Hu Y, Zhu G Y, Chen R P, Tie Z X, Liu J, Jin Z. Highly efficient overall water splitting driven by all-inorganic perovskite solar cells and promoted by bifunctional bimetallic phosphide nanowire arrays[J]. J. Mater. Chem. A, 2018, 6(41): 20076-20082.

[21] Liang J, Liu J, Jin Z. All-inorganic halide perovskites for optoelectronics: progress and prospects[J]. Sol. RRL, 2017, 1(10): 1700086.

[22] Liang J, Wang C X, Zhao P Y, Lu Z P, Ma Y, Xu Z R, Wang Y R, Zhu H F, Hu Y, Zhu G Y, Ma L B, Chen T, Tie Z X, Liu J, Jin Z. Solution synthesis and phase control of inorganic perovskites for high-performance optoelectronic devices[J]. Nanoscale, 2017, 9(33): 11841-11845.

[23] Kim J H, Liang P W, Williams S T, Cho N, Chueh C C, Glaz M S, Ginger D S, Jen A K Y. High-performance and environmentally stable planar heterojunction perovskite solar cells based on a solution-processed copper-doped nckel oxide hole-transporting layer[J]. Adv. Mater., 2015, 27(4): 695-701.

[24] Ameen S, Rub M A, Kosa S A, Alamry K A, Akhtar M S, Shin H S, Seo H K, Asiri A M, Nazeeruddin M K. Perovskite solar cells: influence of hole transporting materials on power conversion eefficiency[J]. ChemSusChem, 2016, 9(1): 10-27.

[25] Jeon N J, Lee H G, Kim Y C, Seo J, Noh J H, Lee J, Seok S I. o-Methoxy substituents in Spiro-OMeTAD for efficient inorganic – organic hybrid perovskite solar cells [J]. J. Am. Chem. Soc., 2014, 136(22): 7837-7840.

[26] Dualeh A, Moehl T, Nazeeruddin M K, Grätzel M. Temperature dependence of transport properties of Spiro-MeOTAD as a hole transport material in solid-state dye-sensitized solar cells[J]. ACS Nano, 2013, 7(3): 2292-2301.

[27] Schölin R, Karlsson M H, Eriksson S K, Siegbahn H, Johansson E M J, Rensmo H. Energy level shifts in spiro-OMeTAD molecular thin films when adding Li-TFSI[J]. J. Phys. Chem. C, 2012, 116(50): 26300-26305.

[28] Wang Y M, Qu H, Zhang C M, Chen Q. Rapid oxidation

of the hole transport layer in perovskite solar cells by a low-temperature plasma[J]. Sci. Rep., 2019, 9(1): 459.

[29] Nouri E, Wang Y L, Chen Q, Xu J J, Dracopoulos V, Sygellou L, Xu Z X, Mohammadi M R, Lianos P. The beneficial effects of mixing spiro-OMeTAD with n-butyl-substituted copper phthalocyanine for perovskite solar cells[J]. Electrochim. Acta, 2016, 222: 1417-1423.

[30] Nguyen W H, Bailie C D, Unger E L, McGehee M D. Enhancing the hole-conductivity of Spiro-OMeTAD without oxygen or lithium salts by using Spiro (TFSI)$_2$ in perovskite and dye-sensitized solar cells[J]. J. Am. Chem. Soc., 2014, 136(31): 10996-11001.

[31] Liu G L, Xi X, Chen R L, Chen L P, Chen G Q. Oxygen aging time: A dominant step for spiro-OMeTAD in perovskite solar cells[J]. J. Renew. Sustain. Ener., 2018, 10 (4): 043702.

[32] Wang H X, Cao S L, Yang B, Li H Y, Wang M, Hu X F, Sun K, Zang Z G. NH_4Cl - modified ZnO for high-performance $CsPbIBr_2$ perovskite solar cells via low-temperature process[J]. Sol. RRL, 2019, 4(1): 1900363.

[33] Guo Y X, Yin X T, Liu J, Que W X. Highly efficient $CsPbIBr_2$ perovskite solar cells with efficiency over 9.8% fabricated using a preheating-assisted spin-coating method [J]. J. Mater. Chem. A, 2019, 7(32): 19008-19016.

[34] Lu J J, Chen S C, Zheng Q D. Defect passivation of $CsPbIBr_2$ perovskites for high-performance solar cells with large open-circuit voltage of 1.28 V[J]. ACS Appl. Energy Mater., 2018, 1(11): 5872-5878.

[35] Zhu W D, Zhang Z Y, Chai W M, Chen D Z, Xi H, Chang J J, Zhang J C, Zhang C F, Hao Y. Benign pinholes in $CsPbIBr_2$ absorber film enable efficient carbon-based, all-inorganic perovskite solar cells[J]. ACS Appl. Energy Mater., 2019, 2(7): 5254-5262.

[36] Liu P Y, Yang X Q, Chen Y H, Xiang H M, Wang W, Ran R, Zhou W, Shao Z P. Promoting the efficiency and stability of $CsPbIBr_2$-based all-inorganic perovskite solar cells through a functional Cu^{2+} doping strategy[J]. ACS Appl. Mater. Interfaces, 2020, 12(21): 23984-23994.

[37] Aristidou N, Eames C, Sanchez-Molina I, Bu X, Kosco J, Islam M S, Haque S A. Fast oxygen diffusion and iodide defects mediate oxygen-induced degradation of perovskite solar cells[J]. Nat. Commun., 2017, 8(1): 15218.

[38] Zhou Y Y, Zhao Y X. Chemical stability and instability of inorganic halide perovskites[J]. Energy Environ. Sci., 2019, 12(5): 1495-1511.

[39] Liu S C, Li Z, Yang Y, Wang X, Chen Y X, Xue D J, Hu J S. Investigation of oxygen passivation for high-performance all-inorganic perovskite solar cells[J]. J. Am. Chem. Soc., 2019, 141(45): 18075-18082.

[40] Tian Y X, Peter M, Unger E, Abdellah M, Zheng K, Pullerits T, Yartsev A, Sundström V, Scheblykin I G. Mechanistic insights into perovskite photoluminescence enhancement: light curing with oxygen can boost yield thousandfold[J]. Phys. Chem. Chem. Phys., 2015, 17(38): 24978-24987.

[41] Brenes R, Guo D, Osherov A, Noel N K, Eames C, Hutter E M, Pathak S K, Niroui F, Friend R H, Islam M S, Snaith H J, Bulovic V, Savenije T J, Stranks S D. Metal halide perovskite polycrystalline films exhibiting properties of single crystals[J]. Joule, 2017, 1(1): 155-167.

[42] Zarazua I, Bisquert J, Garcia-Belmonte G. Light-induced space-charge accumulation zone as photovoltaic mechanism in perovskite solar cells[J]. J. Phys. Chem. Lett., 2016, 7(3): 525-528.

[43] Almora O, Zarazua I, Mas-Marza E, Mora-Sero I, Bisquert J, Garcia-Belmonte G. Capacitive dark currents, hysteresis, and electrode polarization in lead halide perovskite solar cells[J]. J. Phys. Chem. Lett., 2015, 6(9): 1645-1652.

[44] Correa-Baena J P, Turren-Cruz S H, Tress W, Hagfeldt A, Aranda C, Shooshtari L, Bisquert J, Guerrero A. Changes from bulk to surface recombination mechanisms between pristine and cycled perovskite solar cells[J]. ACS Energy Lett., 2017, 2(3): 681-688.

[45] Subhani W S, Wang K, Du M Y, Wang X L, Liu S Z. Interface-modification-induced gradient energy band for highly efficient $CsPbIBr_2$ perovskite solar cells[J]. Adv. Energy Mater., 2019, 9(21): 1703785.

[46] Burschka J, Dualeh A, Kessler F, Baranoff E, Cevey-Ha N L, Yi C, Nazeeruddin M K, Grätzel M. Tris(2-(1H-pyrazol-1-yl)pyridine)cobalt(III) as p-Type dopant for organic semiconductors and its application in highly efficient solid-state dye-sensitized solar cells [J]. J. Am. Chem. Soc., 2011, 133(45): 18042-18045.

[47] Guillén E, Ramos F J, Anta J A, Ahmad S. Elucidating transport-recombination mechanisms in perovskite solar cells by small-perturbation techniques[J]. J. Phys. Chem. Lett., 2014, 118(40): 22913-22922.

[48] Yadav P, Alotaibi M H, Arora N, Dar M I, Zakeeruddin S M, Grätzel M. Influence of the nature of a cation on dynamics of charge transfer processes in perovskite solar cells[J]. Adv. Funct. Mater., 2018, 28(8): 1706073.

[49] Abate A, Leijtens T, Pathak S, Teuscher J, Avolio R, Errico M E, Kirkpatrik J, Ball J M, Docampo P, McPherson I, Snaith H J. Lithium salts as “redox active” p-type dopants for organic semiconductors and their impact in solid-state dye-sensitized solar cells [J]. Phys. Chem. Chem.

Phys., 2013, 15(7): 2572-2579.

[50] Correa-Baena J P, Abate A, Saliba M, Tress W, Jesper Jacobsson T, Grätzel M, Hagfeldt A. The rapid evolution of highly efficient perovskite solar cells[J]. Energy Environ. Sci., 2017, 10(3): 710-727.

[51] Correa-Baena J P, Anaya M, Lozano G, Tress W, Domanski K, Saliba M, Matsui T, Jacobsson T J, Calvo M E, Abate A, Grätzel M, Míguez H, Hagfeldt A. Unbroken perovskite: interplay of morphology, electro-optical properties, and ionic movement[J]. Adv. Mater., 2016, 28(25): 5031-5037.

[52] Pérez-del-Rey D, Forgács D, Hutter E M, Savenije T J, Nordlund D, Schulz P, Berry J J, Sessolo M, Bolink H J. Strontium insertion in methylammonium lead iodide: long charge carrier lifetime and high fill-factor solar cells [J]. Adv. Mater., 2016, 28(44): 9839-9845.

$CsPbIBr_2$ 钙钛矿太阳能电池中通过氧气诱导 Spiro-OMeTAD 快速氧化

王伟国,白 天,薛高飞,叶美丹*

(厦门大学物理科学与技术学院,生物仿生及软物质研究院,物理系,福建省柔性功能材料重点实验室,福建 厦门 361005)

摘要: Spiro-OMeTAD 是钙钛矿型太阳能电池中应用最广泛的空穴传输材料,它本身的空穴传输率很低,需要氧化之后才能满足高效率太阳能电池器件的要求。然而,Spiro-OMeTAD 在空气中的氧化时间较长,同时空气中的水分会造成器件效率的下降以及器件质量不稳定等不良后果。基于此,我们通过一步法制备 $CsPbIBr_2$ 无机钙钛矿太阳能电池,并将旋涂了 Spiro-OMeTAD 层的器件放在纯氧气中氧化,避免因水分导致的钙钛矿层分解。实验结果表明,氧气氧化后的器件最高效率为 7.19%,高于空气中氧化的器件达到的最高效率 6.29%,并且氧气氧化可以将 Spiro-OMeTAD 的氧化时间从 18 小时缩短到 5 小时。我们采用一系列电化学表征方法探讨了不同氧化条件下电池器件的性能差异.结果显示,纯氧气氧化 Spiro-OMeTAD 可以有效减低载流子复合,提高电荷传输。此外,我们采集了多个样本统计分析,发现采用氧气氧化的器件平均效率更高,器件质量更稳定,具有更好的可重复性。这种快速稳定的氧化方法为钙钛矿型太阳能电池的商业化开发提供了有效的思路。

关键词: 钙钛矿;Spiro-OMeTAD;快速氧化;$CsPbIBr_2$;太阳能电池